

A novel amplitude-equalized all-optical clock recovery scheme

F. WANG^{a, b}, X. L. ZHANG^b, Y. YU^b, Z. ZHANG^b

^a*School of Mathematics and Physics, Chongqing Institute of Technology, Chongqing 400050, P. R. China*

^b*Wuhan National Laboratory for Optoelectronics & School of Optoelectronic Science and Engineering, Huazhong University of Science and Technology, Wuhan, 430074, P. R. China*

We presented a novel all-optical clock recovery scheme based on nonlinear polarization rotation (NPR) in a semiconductor optical amplifier (SOA) ring fiber laser for acquiring amplitude-equalized clock from input pseudo-random bit sequence (PRBS) return-to-zero (RZ) signal. Adjusting polarization direction of optical field in ring cavity, the reflective SOA together with the polarization beam splitter (PBS) can function as a saturable transmitter, where a high peak power is depressed and a low peak power is enhanced, amplitude ripple of recovered clock can be suppressed effectively. Clock amplitude jitter (CAJ) of recovered clock is lower than 1.5 % over a 25 nm tuning range.

(Received February 8, 2008; accepted April 2, 2008)

Keywords: All-optical clock recovery, Mode-locked fiber ring laser, Birefringence, Nonlinear polarization rotation (NPR), Reflective semiconductor optical amplifier (RSOA)

1. Introduction

In future high-speed optical networks, all-optical signal processing schemes are likely to be used. One of the most pressing problems is clock recovery (CR), which is a vital ingredient for many key functions such as 3R regeneration, all-optical demultiplexer, and so on. In recent years, a number of CR techniques have been demonstrated, which include optical phase-locked loops [1-3], self-pulsating distributed feedback (DFB) lasers [4-6], and synchronized mode-locked fiber ring lasers [7-8]. CR in a fiber ring laser actively mode-locked by the injection optical data stream permit tuning and switching of the wavelength, moreover, clock division and multiplication can be obtained easily, which has received much attention. In this technique, the semiconductor optical amplifier (SOA) was used frequently, acted as injection mode-locker. However, because the recovery time of the carrier density in the SOA is about several hundred picoseconds, the amplitudes of the clock inevitably fluctuate along with the injected data pattern and the center times of the pulses also jitter seriously. Some methods had been presented to alleviate these effects [8, 9]. In this letter, we propose a novel method where nonlinear polarization rotation (NPR) in a reflective semiconductor optical amplifier (RSOA) is utilized to overcome the pattern effect in recovered clock.

2. Experimental setup and principle

Fig. 1 depicts the experimental setup of all-optical CR based on NPR in a mode-locked fiber ring laser. A pseudorandom bit sequence (PRBS) return-to-zero (RZ) signal is generated by modulating CW emitted by a distributed-feedback laser diode (DFB-LD) using two LiNbO₃ Mach-Zehnder modulators and its power can be controlled by an erbium-doped fiber amplifier (EDFA) and the attenuator (ATT). CR unit is formed by a conventional

SOA (CSOA), a RSOA, two circulators, two polarization controllers (PCs), a polarization beam splitter (PBS), a band pass filter (BPF), an isolator, an optical delay line (ODL), and a 90:10 coupler. Gain of CSOA is depleted by the backward injecting optical signal, and it acts as an active modulator, whereas, polarization-dependent RSOA together with following PBS introduces NPR effect to acquire clock-amplitude equalization. PC₁ is used to adjust the angle between polarization state of the input signal and TM mode of the RSOA. PC₂ is used to adjust the polarization of the amplified SOA output with the orientation of PBS.

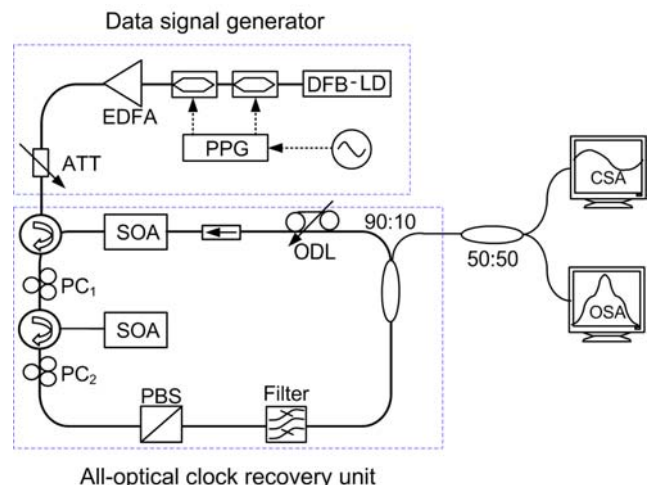


Fig. 1. Experimental setup for all-optical CR.

We can assume that NPR primarily occurs in RSOA. The incoming polarized electric field is decomposed into TE component (electric field parallel to the layers in the waveguide of SOA) and TM component (electric field perpendicular to the layers in the waveguide), the

corresponding components on the TE axis and TM axis of RSOA can be given as follows:

$$E^{TE} = E \cos \alpha_1 e^{i\phi_{x0}}, E^{TM} = E \sin \alpha_1 e^{i\phi_{y0}} \quad (1)$$

Where, E represents the linear polarized electric field before entering into RSOA, α_1 is the angle between TM axes of the RSOA and polarization direction of input signal, ϕ_{x0} and ϕ_{y0} are initial phase of input signal for TE mode and TM mode, respectively. The spatially varying component of the field in RSOA can be decomposed into forward E^+ and backward-propagating wave E^- , and the traveling-waving equation for TE mode and TM mode are given by [10]

$$\left(\frac{\partial}{\partial t} + v_g^{TE} \frac{\partial}{\partial z}\right) E^{TE\pm}(z, t) = \frac{1}{2} \Gamma^{TE} (1 + i\alpha) g^{TE}(z, t) E^{TE\pm}(z, t) - \frac{1}{2} \alpha_s E^{TE\pm}(z, t) \quad (2)$$

$$\left(\frac{\partial}{\partial t} + v_g^{TM} \frac{\partial}{\partial z}\right) E^{TM\pm}(z, t) = \frac{1}{2} \Gamma^{TM} (1 + i\alpha) g^{TM}(z, t) E^{TM\pm}(z, t) - \frac{1}{2} \alpha_s E^{TM\pm}(z, t) \quad (3)$$

Where, v_g is the corresponding group velocity taken at the central frequency of the wave, Γ is the confinement factor, $g(z, t)$ is the gain function, α is the phase-modulation parameter, and α_s is the internal absorption. The nonlinear phase of TE and TM mode can be expressed as

$$\Phi^{TE}(z, t) = \frac{1}{2} \alpha (\ln(G^{TE}(z, t)) + \alpha_s z) \quad (4)$$

$$\Phi^{TM}(z, t) = \frac{1}{2} \alpha (\ln(G^{TM}(z, t)) + \alpha_s z) \quad (5)$$

Where, $G^{TE}(z, t)$, $G^{TM}(z, t)$ is modal gain of the SOA along the TE axes and the TM axes, respectively. The boundary conditions at rear facet for input signal can be expressed as

$$\begin{aligned} E^{TE-}(L, t) &= E^{TE+}(L, t)r, \\ E^{TM-}(L, t) &= E^{TM+}(L, t)r. \end{aligned} \quad (6)$$

Where, L is length of SOA, r is the reflectivity coefficient of rear facet. The output electric field corresponding to output polarizer placement angle of α_2 is

$$E_{0,out} = E^{TE-}(0, t) \cos \alpha_2 + E^{TM-}(0, t) \sin \alpha_2 \quad (7)$$

Hence, the output intensity I_{out} is given as

$$I_{out}(t) = E_{0,out} \cdot E_{0,out}^* \quad (8)$$

i.e.

$$\begin{aligned} I_{out}(t) &= I_{in}(t) \cos^2 \alpha_1 \cos^2 \alpha_2 \times (G^{TE}(0, t) \\ &\quad + 2\sqrt{G^{TE}(0, t)G^{TM}(0, t)} \tan \alpha_1 \tan \alpha_2 \cos(\phi_{diff}(0, t) + \phi_{PC}) \\ &\quad + G^{TM}(0, t) \tan^2 \alpha_1 \tan^2 \alpha_2) \end{aligned} \quad (9)$$

Where, $I_{in}(t)$ is the intensity profile of input optical pulse linearly polarized, $G^{TE}(0, t)$, $G^{TM}(0, t)$ is round-modal-gain of the RSOA along the TE axes and the TM axes, respectively, $\phi_{diff}(0, t)$ is the phase difference between TE and TM modes, and ϕ_{PC} is the phase difference induced by the polarization controller. One can see from (1) that the output signal will depend on the phase difference and SOA gain along TE and TM axes which in turn depends on the magnitude of input power and bias current of SOA [11]. Because TE and TM component collect different intensity-dependent phases and amplitudes, different parts of the output pulse are with different polarization states. By adjusting α_1 and α_2 , under appropriate conditions, the structure will function as a saturable transmitter, wherefore a high peak power is suppressed and a low peak power is enhanced. Therefore, clock-amplitude equalization can be realized in this manner.

3. Results and discussion

The CSOA has a multi-quantum-well (MQW) active region, which can accelerate carrier recovery in high bit rate operation. Its gain is almost polarization-independent. The RSOA has a longer active region (1000 μm), and its rear-facet reflectivity is 30 %. The RSOA exhibits 10dB polarization gain dependence. The PBS has an extinction ratio of 20 dB and the tunable filter has a FWHM-bandwidth of 1 nm. The total cavity length of the commercially available fiber-pigtailed components is about 20 m. Bias current of CSOA and RSOA is 180 mA and 250 mA, respectively.

Fig. 2a shows the eye diagram of the input 10Gbit/s PRBS-RZ signal at 1563.65 nm. Average power of the RZ signal is 5 dBm. From Fig. 2a, we can see that quality of the data signal is not good, the pulse amplitude is uneven and pulse width is also different. It is caused by the noise from LD and EDFA and the unapt current bias of the modulators. If there is no PBS and PC₂ in the ring cavity, there is no NPR effect. Under this condition, a 10 GHz recovered clock train at 1560.07 nm is shown in Fig. 2b. In spite of pulse width is compressed and extinction ratio (ER) is enhanced comparing with input PRBS-RZ signal, but, clock pulse amplitude is uneven. It is explained as that the spontaneous emission in SOA is modulated by the not well input signal via cross-gain modulation (XGM) effect.

When PBS and PC₂ are inserted into the cavity, NPR will take effect. The recovered clock signal and corresponding optical spectrum is presented in Fig. 2c and Fig. 2d, respectively. The average optical pulsewidth and root-mean-square timing jitter measured by the oscilloscope are 20 ps and 1.5 ps respectively. The wavelength of the recovered clock signal is 1560.07 nm and the 3 dB spectral width is about 0.42 nm. Thus the time bandwidth product of the recovered optical pulse train is over 1.0, far from the transform limit.

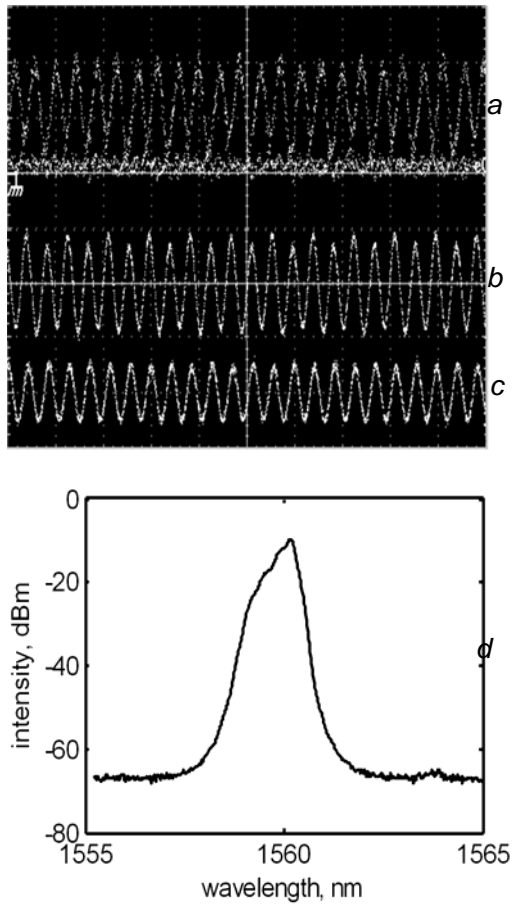


Fig. 2. Eye-diagram (100ps/div), a PRBS RZ signal at 1563.65 nm, b Recovered clock train without clock amplitude equalization, c Recovered clock train with clock amplitude equalization, d Optical spectrum corresponding to c.

We also investigate wavelength tunability of recovered clock. Fig. 3 show recovered clock trains at different wavelengths. In Fig. 3a~e, the wavelength of the recovered clock signal is 1540.44 nm, 1545.52 nm, 1551.22 nm, 1555.17 nm, and 1566.37 nm, respectively. The average power and the clock amplitude jitter (CAJ) of recovered clock at different wavelengths are shown in Fig. 4. With Varying to long wavelength, the average power of recovered clock increase and CAJ is always lower than

1.5 %.

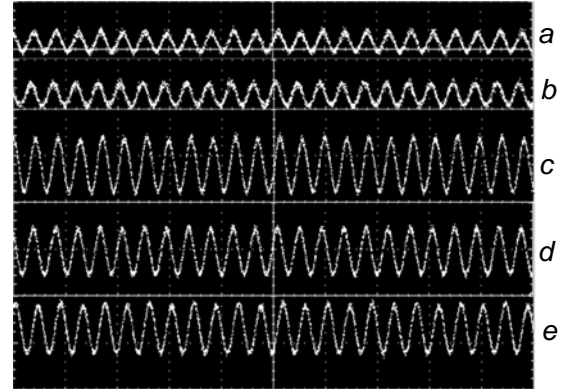


Fig. 3. Recovered clock trains with clock amplitude equalization at different wavelengths (100ps/div).

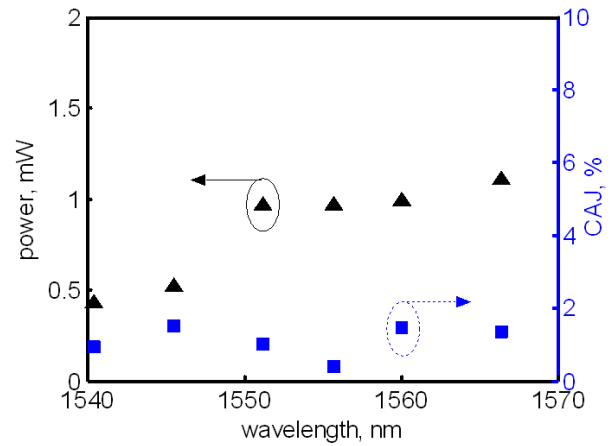


Fig. 4. The average power and the CAJ of recovered clock at different wavelengths.

4. Conclusion

Amplitude-equalized clock recovery based on NPR of RSOA in a mode-locked ring fiber laser has been proposed and successfully demonstrated. By adjusting PCs, CAJ of recovered clock signal is always lower than 1.5 % over a 25 nm tuning range.

Acknowledgements

This work is supported by National High Technology Developing Program of China (Grant No. 2006AA03Z0414), the Science Fund for Distinguished Young Scholars of Hubei Province (Grant No. 2006ABB017) and the Program for New Century Excellent Talents in Ministry of Education of China (Grant No. NCET-04-0715). The authors also gratefully acknowledge the support from the Commission of Science and Technology of Chongqing City of P. R. China (CSTC, 2006BB2405).

References

- [1] H. Dong, H. Z. Sun, G. H. Zhu, Q. Wang, N. K. Dutta, *Opt. Express*, 2004, **12**(20), 4751 (2004).
- [2] G. Zhu, Q. Wang, H. Chen, N. Dutta, *J. Opt. Engineering*, **43**, 1056 (2004).
- [3] O. Kamatani, S. Kawanishi, *IEEE Photonics Technol. Lett.* **8**(8), 1094 (1996).
- [4] C. Bornholdt, B. Sartorius, S. Schelhase, M. Mohrle, S. Bauer, *Electron. Lett.* **36**(4), 327 (2000).
- [5] W. M. Mao, Y. H. Li, M. A. Mumin, G. F. Li, *J. Lightwave Technol.* **20**(9), 1705 (2002).
- [6] Y. H. Li, C. Kim, G. F. Li, Y. Kaneko, R. L. Jungerman, O. Buccafusca, *IEEE Photonics Technol. Lett.* **15**(4), 590 (2003).
- [7] K. Vlachos, K. Zoiros, T. Houbavlis, H. Avramopoulos, *IEEE Photon. Technol. Lett.* **12**(1), 25 (2000).
- [8] D. M. Patrick, R. J. Manning, *Electron. Lett.* **30**(2), 151 (1994).
- [9] K. Vlachos, G. Theophilopoulos, A. Hatziefremidis, H. Avramopoulos, *IEEE Photon. Technol. Lett.* **12**(6), 705 (2000).
- [10] H. J. S. Dorren, D. Lenstra, Y. Liu, M. T. Hill, G. D. Khoe, *IEEE J. Quantum Electron.* **39**(1), 141 (2003).
- [11] B. S. G. Pillai, M. Premaratne, D. Abramson, K. L. Lee, A. Nirmalathas, C. Lim, S. Shinada, N. Wada, T. Miyazaki, *IEEE J. Quantum Electron.* **42**(10), 1062 (2006).

* Corresponding author: wangf17@cqit.edu.cn